

Submerged Friction Stir Welding of 6061-T6 Aluminium Alloy under Different Water Heads

Rathinasuriyan Chandran^{a*}, Senthil Kumar Velukkudi Santhanam^b

^aDepartment of Mechanical Engineering, Adhi College of Engineering and Technology, Chennai, India

^bDepartment of Mechanical Engineering, CEG, Anna University, Chennai, India

Received: December 07, 2017; Revised: August 20, 2018; Accepted: September 28, 2018

The aim of this paper is to determine the feasibility of submerged friction stir welding of 6061-T6 aluminium alloy on different water heads through macrostructural analysis. In this work, aluminium 6061-T6 alloy was friction stir welded under normal and submerged conditions at different rotational speeds of 400 rpm, 800 rpm, 1200 rpm, 1600 rpm. The water head was varied from 10 to 30 mm in the case of the submerged friction stir welding process. In both normal and submerged friction stir welding processes, a welding speed of 45 mm/min, a normal load of 30 kN, tool tilt angle of 2°, depth of tool penetration and tool geometry were kept constant. Torque is measured during the welding process, and power (kW) is calculated after the welding process. The macrostructural analysis was carried out for locating defect formation and identifying the feasible working range of process parameters of the welded aluminium 6061-T6 alloy. The mechanical properties such as ultimate tensile strength and microhardness of submerged friction stir welded of 6061 aluminium alloys were investigated. Scanning Electron Microscope (SEM) metallography was used for comparing the microstructure of the parent material, friction stir welded and submerged stir welded samples.

Keywords: Friction Stir Welding (FSW), Submerged Friction Stir Welding (SFSW), Microstructure, Mechanical Properties.

1. Introduction

Friction Stir Welding (FSW) was invented by The Welding Institute (TWI), the UK during the 1990s. In FSW, a non-consumable rotating tool with a pin and a shoulder are inserted into plates to be joined at a specific load, rotational and welding speed¹. Heat treatable aluminium alloys with good strength to weight ratios are commonly used in aircraft and aerospace applications². In recent years, some of the researchers have used water to friction stir weld the various aluminium alloys³⁻⁷. In Submerged Friction Stir Welding (SFSW) process, the entire workpiece is immersed in a liquid environment during the friction stir welding. It has achieved greater tensile strength and elongation compared to the typical friction stir welding⁸. Su et al.⁹ used to measure the tool torque, traverse force and axial force for friction stir welding of AA2024-T4 aluminium alloys by the indirect method. The measured value agrees well with the available data captured by the rotation component dynamometers and load cells. Tool torque is indirectly proportional to the tool rotational speed and directly proportional to the welding speed. Traverse force is related to the welding and the tool rotation speeds. The axial force is considerably larger than the traverse force. Caroline Jonckheere et al.¹⁰ have carried out the friction stir welds between the similar/dissimilar of 2014 and the 6061 heat treatable aluminium alloy. Torque, power, and temperature were measured during the welding process, macrographies and hardness profiles were performed

after the welding process. The power inputs of 6061 alloy are forever higher than a 2014 alloy when welding was performed under similar conditions. Abd El-Hafez et al.¹¹ have studied the mechanical properties and the welding power consumption on the 2024-T35 aluminium alloy joints at different rotation speeds, welding speeds, and tool profiles. The welding power consumption was measured and theoretically calculated using two models established by Frigaad and Heurtier. The measured power agrees with theoretical model established by the Heurtier. Lakshminarayanan et al.¹² have developed a friction stir welding window based on macrostructural analysis for the efficient joining of 2219 aluminium alloy. In general, defects are noticed in fusion welding of aluminium alloys like cracks, porosity, slag inclusion, etc. due to the poor solidification. These defects affect the weld quality and joint properties. Friction stir welding is a solid-state welding process; therefore, no melting takes place during the welding process, and so it is free from these defects. However, other defects are noticed in the friction stir welding process like tunnel defect, cracks, pinhole, kissing bond, piping defect, etc. due to inadequate heat generation and material flow of metal. This window is very much useful for selecting the friction stir welding process parameters to acquire defect free joints. They have attained the defect-free joints at the rotational speed range from 700 to 1600 rpm and the welding speed of 30 to 150 mm/min.

Liu Hui-jie et al.¹³ have conducted the underwater friction stir welding of 2219 aluminium alloy for improving the weld properties. Coarsened grain was attained during the normal

*e-mail: rathinasuriyanphd@gmail.com

friction stir welding, which is significantly involved in reducing the hardness. High-density dislocations and refined grain structures were formed in submerged friction stir joint due to the precipitates dissolved in the matrix. This leads to the enhancement of the weld properties such as hardness and tensile strength. Basil Darras et al.¹⁴ has discussed the friction stir processing of AZ31 Magnesium alloy in normal and submerged conditions and their inheritance on tensile properties, grain structure, power consumption, and thermal fields. The average grain size of 18.9 μm , 15.9 μm , and 13.3 μm was attained for FSP in their, submerged in hot water and cold water respectively. More grain refinement was achieved in cold water conditions. Huijie Zhang et al.¹⁵ demonstrated the submerged friction stir welding of 2219-T6 aluminum alloys. In this, rotational and welding speeds are the most important parameters that affect the tensile strength of the welded sample. The ultimate tensile strength of 360 MPa was obtained through SFSW in an optimized condition. This tensile strength value for SFSW is 6% higher than the normal FSW. Emad Eldin Kishta et al.¹⁶ have studied the void fractions, thermal histories, tensile properties, microhardness and power of the submerged friction stir welded 5083 aluminium alloy. The results showed that the submerged friction stir welding produced good weld strength and considerable diminution in the void fraction. Zhang et al.¹⁷ exhibited submerged friction stir welded on 2219-T6 aluminum alloy at a fixed welding speed of 100 mm/min and different rotational speeds of 600, 800, 1000, 1200 and 1400 rpm respectively. The void defect was identified in the stir zone due to the excess heat generation of the welded plates at the higher rotational speed of 1400 rpm. The minimum hardness value was obtained in the SFSW at a rotation speed of too low and too high conditions.

Liu et al.¹⁸ was friction stir welded of 2219 aluminum alloy under the water at a fixed rotational speed of 800 rpm and different welding speeds of 50, 100, 150 and 200 mm/min for finding the effect of welding speed on the mechanical properties of welded plates. The formation of a precipitate is weakened in the thermal mechanically affected zone and the heat affected zone when to increase the welding speed. Tensile strength was increased by varying the welding speed range from 50-150 mm/min decreasing in 200 mm/min due to the formation of groove defect. The lowest hardness value was found in the HAZ at the welding speed of 50 mm/min. When the rotational speed increased from 100 to 150 mm/min, the lowest hardness value was obtained in the TMAZ. Finally, the lower hardness region is moved to the nugget zone of welded of 2219 aluminum alloy at the welding speed of 200 mm/min. Jicheng Gao et al.¹⁹ presents an experimental study on submerged friction stir welding of acrylonitrile butadiene styrene and polycarbonate. They have obtained the minimum tensile strength due to the form of pores, cracks, and voids defects.

Thomas Bloodworth²⁰ carried out submerged friction stir welding of 6061-T6 aluminum alloy under the water. They have reported about the development of gas bubbles during the submerged friction stir welding process. These would create voids in the nugget and thermo-mechanically affected zone as a result of porosity formed. These defects depend very much on the water depth i.e. water level from the surface of the welded sample. Hence, the water head (water depth) parameter is important, and it is taken as one of the submerged friction stir welding process parameters in this work. The objective of this work is to study the feasibility of weld, with submergence of the 6061-T6 aluminium alloy under varied water heads through macrostructural analysis.

2. Experimental Set-up

The weld samples used for the experiment were of 6 mm thickness 6061-T6 aluminium alloy with dimensions of 140 mm length and 70 mm width. Both friction stir and submerged friction stir welding processes were carried out by the non-consumable tool of H13-tool steel with the dimensions of the shoulder diameter of 25mm, pin diameter of 6 mm and pin length is 5 mm respectively, as shown in Fig. 1.

In submerged friction stir welding, the fixture is set into the tank, and the samples are clamped on it. Water is poured into the tank until the water level reaches the top surfaces of the samples and the water temperature 30°C is maintained for all the experiments. The water head is taken into account with the thickness of the gasket sheet and fixture of around 30 mm after which the water head is experimented with 10, 20 and 30 mm respectively. The volume of the water about the first water head is 9 liters. Similarly, it is increased for various water heads. The combinations of the weld parameter are shown in the Table 1.

Friction stir and submerged friction stir welding are performed by a servo controlled FSW machine along a rolling direction of the 6061-T6 aluminium alloy under air and water conditions. In this work, the experiments are conducted while particularly varying the rotational speeds of 400 rpm, 800 rpm, 1200 rpm and 1600 rpm. The parameters, welding speed and axial load are constant. The water heads are varied from 10 mm, 20 mm and 30 mm respectively in

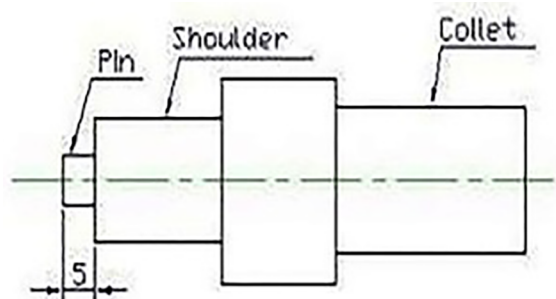


Figure 1 . Schematic view of FSW/SFSW Tool

Table 1. Combinations of weld parameter

Sl.No	Water head(mm)	Rotational speed (rpm)
1	0 (Without water)	400
2		800
3		1200
4		1600
5	10	400
6		800
7		1200
8		1600
9	20	400
10		800
11		1200
12		1600
13	30	400
14		800
15		1200
16		1600

case of submerged friction stir welding process for studying their influence on the welds. Puviyarasan et al.²¹ found that the most influence process parameter as rotational speed during the friction stir processing. This is the reason for particularly varying the rotational speeds.

The measurement methods of torque are classified into two types, such as direct and indirect²². In this work, the value of torque is measured using load cells. The load cells are inbuilt with the friction stir welding machine. The value of torque is continuously measured through direct measurement instruments at intervals of 20 seconds during the experiments. The processing view of the submerged friction welding process is shown in Fig. 2.

After the welding process, the joints are sectioned at a 90-degree angle to the welding direction for metallographic analyses tensile and microhardness tests, using the wire electrical-discharge cutting (WEDM) machine. The cross-section which is taken as welded specimens is polished using various grids and etched with Tucker's reagent by an

**Figure 2 .** Processing view of SFSW

optical microscopy for metallographic analysis. The tensile specimens are prepared according to the ASTM [E8M-04] international codes²³ and some of the tested samples are shown in Fig. 3.

The microhardness (Hv) test was performed at the mid-thickness across the weld zone at 4.9 N load for 10 sec to attain the hardness profiles. The sectioned specimens were polished with a diamond paste, etched with Keller's reagent and observed on Scanning Electron Microscope (SEM).

3. Result and Discussions

3.1 Torque

3.1.1. Without water head

The variation of torque (Nm) generation is established for every 20 sec at different rotation speeds of 400, 800, 1200 and 1600 rpm under the normal friction stir welding (without water head) conditions as shown in Fig. 4. The maximum torques in the friction stir welding of 37.7, 23.3, 17.5 and 13.8 Nm are found at the rotational speed rates of 400, 800, 1200 and 1600 rpm. The maximum torque is obtained at a low rotational speed of 400 rpm. It renders the material difficult to soften so that torque generation is high at the low rotational speed 400 rpm. The minimum torque is obtained at a high rotational speed of 1600 rpm as the making of material is softer and too easy due to high heat generation. As a result, the torque generation is high at the higher rotational speed of 1600 rpm. Finally, the torque increases with a decrease in rotational speed.

3.1.2. Water head of 10 mm

The deviation of torque (Nm) value is noted for every 20 sec at different rotation speeds of 400, 800, 1200 and 1600 rpm under the submerged friction stir welding (water head is 10 mm) conditions as shown in Fig. 5.

The maximum torque established are 89.1, 53.4, 37.2 and 31.6 Nm at the rotational speed rates of 400, 800 and 1200 and 1600 rpm. The torque value increases with a decrease in tool rotational speed. The torque value is higher in comparison to the normal friction stir welding. In this condition, the heat generation of the weld is expected low when compared to the normal friction stir welding. It makes the material difficult to soften and may lead to an increase in the torque value.

3.1.3. Water head of 20 mm

The variations in torque (Nm) with sliding time of 20 sec for different rotation speeds of 400, 800, 1200 & 1600 rpm at water head of 20 mm details are shown in Fig. 6.

The maximum torque values 94.7, 54.4, 41 and 32.3 Nm are observed at the speed rates of 400, 800, 1200 and 1600 rpm. The torque value is higher again when compared to the submerged friction stir welding at the water head of 10 mm. Heat generation is very low in this state due to the



Figure 3 . Tensile specimen

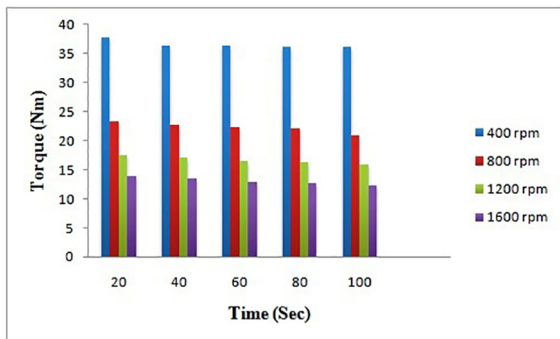


Figure 4 . Torque on the welds without water head (normal FSW) at the rotational speed rates of 400, 800, 1200 and 1600 rpm

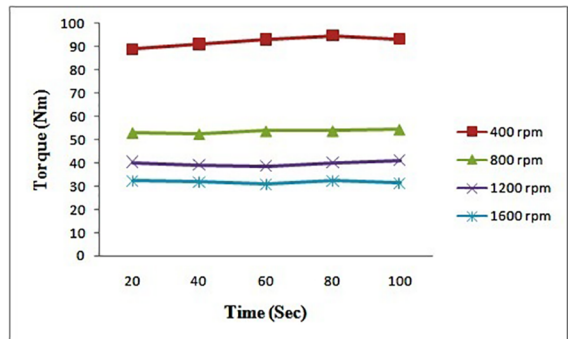


Figure 6 . Torque on the welds with water head of 20 mm and rotational speed rates of 400, 800, 1200 and 1600 rpm

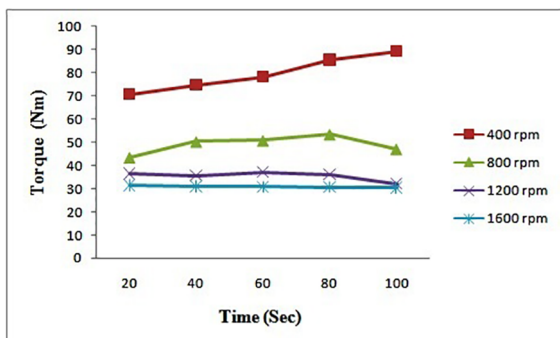


Figure 5 . Torque on the welds with water head of 10 mm at the rotational speed rates of 400, 800, 1200 and 1600 rpm

use of a quantity of water being high when compared to the submerged friction stir welding at the water head of 10 mm and it may cause an increase in torque.

3.1.4. Water head of 30 mm

The torque generation (Nm) on the welds of water head 30 mm at rotational speed rates of 400, 800 and 1200 and 1600 rpm are shown in Fig.7.

The maximum torque values obtained are 95.7, 56, 39.5 and 33.42 Nm at the rotational speed rates of 400, 800, 1200 and 1600 rpm. Around 13.5 liters of water is used at this condition due to which, the water cooling action is high with low heat generation compared to the water head of 20

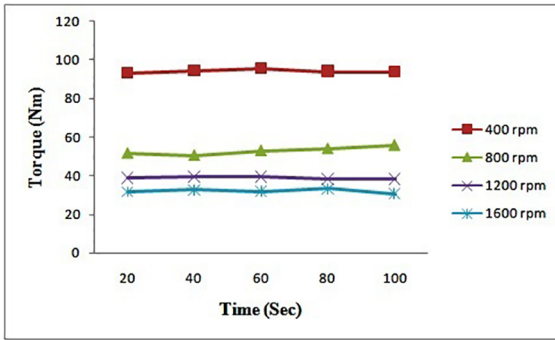


Figure 7. Torque on the welds with water head of 30 mm and tool rotational speed rates of 400, 800, 1200 and 1600 rpm

mm. It results in increase of the torque. In this work, the torque is high during submerged conditions when compared to the normal FSW. Thomas Bloodworth²⁰ reported that the torque values of normal/submerged friction stir welding were 16 Nm and 18.5 Nm respectively. The torque value is higher by 14.5% during SFSW when compared to NFSW. It was expected that the generation of frictional heat would go into the heating of the water.

3.2 Power

Power (W) is calculated¹¹ from the following equation (1),

$$P = \frac{2\pi\omega M}{60} \quad (1)$$

Where P- Power (watts); ω - rotational speed (rpm); M-Torque

The results of the weld power (watts) on the welds produced in the absence of water head (normal FSW) and with water head (SFSW) of 10, 20 & 30 mm at the rotational speed rates of 400, 800, 1200 and 1600 rpm are represented in Fig.8 (a-d).

The maximum power consumed 2.3, 5.3, 5.4 and 5.6 kW are observed without water head (normal FSW) and with water head (10, 20 & 30 mm) conditions. With both friction and submerged friction stir welding processes, the maximum power is found at the higher rotational speed rates of 1600 rpm and the minimum power is found at the lower rotational speed rates of 400 rpm. The consumed weld power of submerged friction stir welding process was higher than the normal friction stir welding process; this happened due to the difficulty seen in softening the material during the submerged friction stir welding process. This could lead to an increase in the weld power in the submerged friction stir welding process.

3.3 Macrostructural analysis

A total of sixteen joints are fabricated for the study of the effect and weld quality on normal and submerged friction stir welded AA6061-T6 alloy. Four joints were fabricated; welding speed and axial force are invariable while varying the

rotational speed in the normal friction stir welding process. The remaining twelve joints were fabricated; welding speed and axial force were kept constant while varying the rotational speed and water head in the submerged friction stir welding process. The macrostructure of the friction stir and submerged friction stir welded of AA6061-T6 aluminium alloy at different rotational speed, and water head is displayed in Table 2.

Defects such as tunneling effect, poor stirring, wormhole and pinhole are identified at the rotational speed of 400 rpm with both normal friction stir/submerged friction stir welding processes due to the insufficient material flow caused by inadequate heat generation.

The best weld morphology, without defects, is achieved in normal friction welding at the rotational speed of 800 and 1200 rpm due to adequate heat generation of welded material. Elatharasan et al.²⁴ were carried out the friction stir welding process of AA 6061-T6 aluminum alloy by the central composite design (CCD) matrix. They have also identified the working range of rotational speed from 800 rpm to 1200 rpm.

In the case of the submerged friction welding process, the best weld morphology was achieved for the water head of 10, 20 and 30 mm at the rotational speed from 800 to 1600 rpm due to the adequate heat generation and adequate flow of material. The superior weld morphology of onion ring pattern was achieved in submerged friction welding at the rotational speed of 1200 rpm under the water head of 10, 20, 30 mm, and at the rotational speed of 1600 rpm under the water head of 30 mm respectively. This is due to the optimized heat generation and cooling in these process. An onion skin means the semicircular pattern is formed on the surface of the welded sample during the welding process, and the different bands in the weld nugget zone (SZ) are called onion rings. It is a significant feature of the nugget zone in friction stir welded or processed samples²⁵. The onion rings were formed on the weld nugget zone due to the incessant movement of materials by the pin when the welding speed is lower, and the rotational speed is higher²⁶.

3.4 Tensile properties

Figure 9 describes the plots against rotational speed and the tensile strength of the friction stir and submerged friction stir welds under the water head of 10, 20 & 30 mm on AA6061-T6 alloy. During NFSW, the tensile strength was found as 144 MPa at the rotational speed of 400 rpm. At the rotational speed of 800-1200 rpm, the tensile strength also increased to 158 MPa and 182 MPa respectively. With increasing the rotational speed of 1600 rpm, the tensile strength decreased to a low value of 151 MPa due to the excess heat input. The excess heat input was induced by increasing the fluidity of the material, and results made the turbulence flow in the weld nugget zone during friction stir welding. Finally, it causes the formation of the defect and also reduces the tensile strength¹⁷.

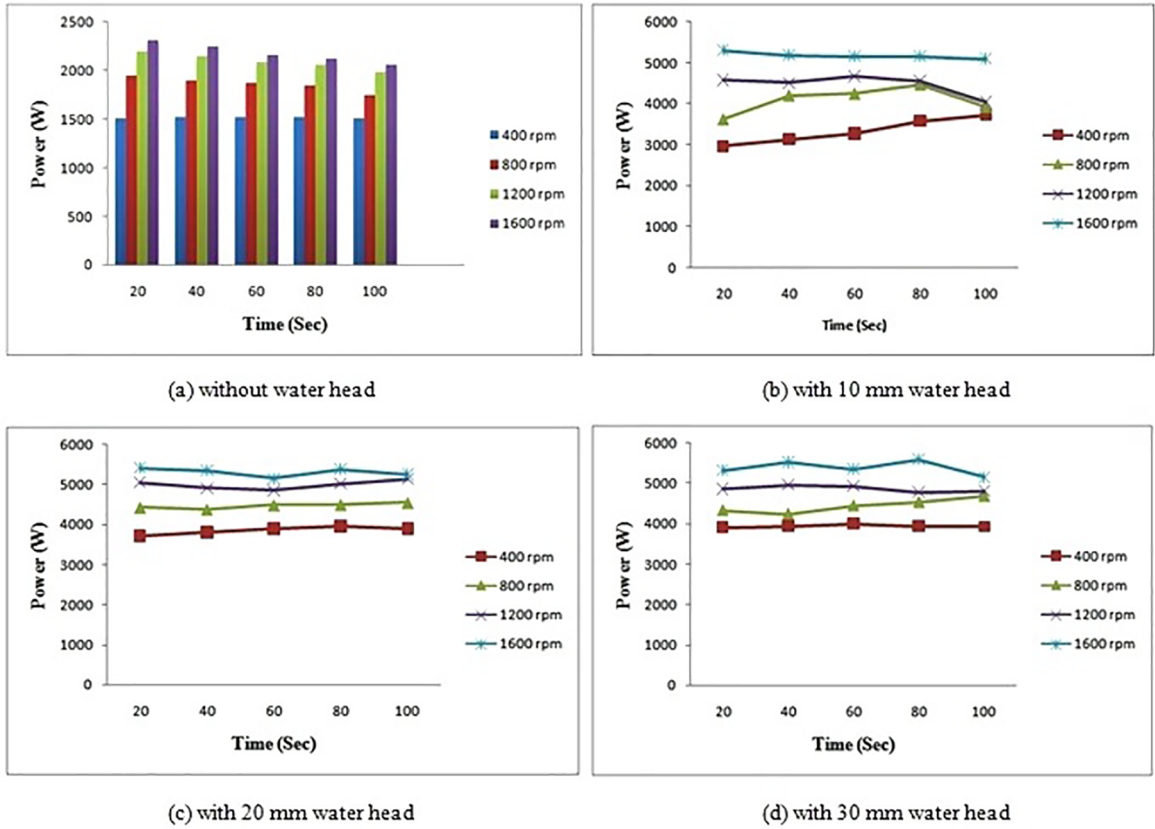


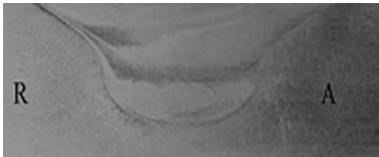

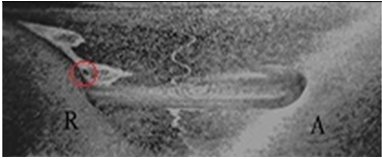

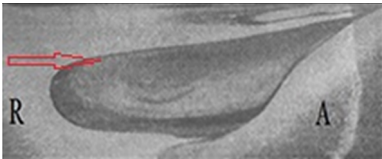



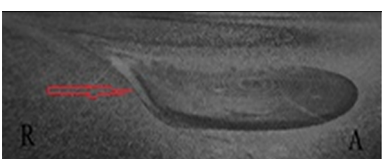


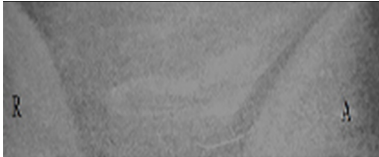




Figure 8 . Weld power on the welds (a) without water head (b) with 10 mm water head (c) with 20 mm water head (d) with 30 mm water head

Table 2. Macrostructure observation of 6061-T6 aluminium alloy

Water head(mm)	Rotational speed (rpm)	Macrography	Weld defects	Probable reason
Nil	400		Tunneling effect at the middle	Inadequate heat input and insufficient material flow
	800		No defects	Adequate heat input and also adequate material flow
	1200		No defects	Adequate heat input and as well adequate material flow
	1600		Worm hole at the middle and top	Excess heat input per unit length of the weld

Water head(mm)	Rotational speed (rpm)	Macrography	Weld defects	Probable reason
10	400		Pin hole	Low heat generation
	800		No defects	Enough heat input
	1200		No defect (onion ring at the advancing side)	Proper heat input and cooling effect
	1600		No defects	Sufficient heat input and cooling effect
	400		Tunneling effect at the middle	Insufficient heat input
20	800		No defects	Sufficient heat input
	1200		No defects (onion ring pattern with strongly at the retreating side)	Optimized heat input as well as cooling effect
	1600		No defects (onion ring pattern at the advancing side)	Proper heat input as well as cooling effect

Water head(mm)	Rotational speed (rpm)	Macrography	Weld defects	Probable reason
30	400		Poor stirring	Lack of sufficient material flow
	800		No defects	Sufficient heat input
	1200		No defects (onion ring pattern at the advancing side)	Appropriate heat input and cooling effect
	1600		No defects	An adequate amount of heat input

The maximum tensile strength (MPa) of 207, 218 and 211 MPa were found during submerged friction stir welding condition at the rotational speed of 1200 rpm in the water head of 10, 20 and 30 mm. In this work, the maximum tensile strength was found at the rotational speed of 1200 rpm in the water head of 20 mm which was supported by the formation of onion ring pattern strongly. Also, during submerged friction stir welding process, the tensile strength of the welded plate first increased from 400 to 1200 rpm, but it is decreased in 1600 rpm. Zhang et al.¹⁷ have found identical results. They have reported that increasing the tensile properties first from 600 to 800 rpm, reducing reaches a plateau between 800 and 1200 rpm later and then decreased the tensile strength at 1400 rpm. The tensile strength of the submerged friction stir joints was higher than that of the normal friction stir joints due to the positive effect of water cooling action of 6061-T6 aluminum alloys. The poor tensile strength was found at the lower rotational speed of 400 rpm, due to the formation of tunneling defect and inadequate heat generation. The maximum tensile strength was found at the rotational speed of 1200 rpm due to adequate heat generation and proper cooling effect. The refined grain size and high-density dislocations lead to the increase the mechanical properties like tensile and hardness¹³. The tensile strength improved in submerged friction stir welding process due to the controlling of temperature and microstructural evolutions¹⁵.

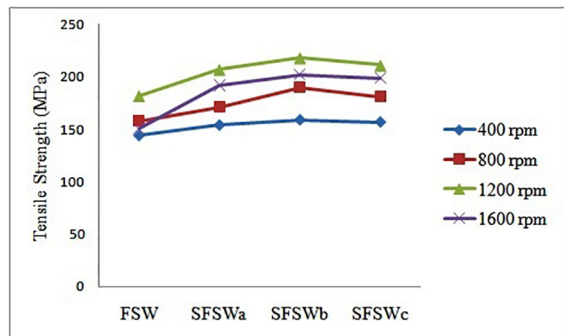


Figure 9. Tensile properties of FSW and SFSW (SFSWa - Submerged friction stir welding for 10 mm water head; SFSWb - Submerged friction stir welding for 20 mm water head; SFSWc - Submerged friction stir welding for 30 mm water head; FSW - Friction stir welding for without water head)

3.5 Hardness

The microhardness (Hv) profiles of the transversal section of friction stir and submerged friction stir weld from the water head of 10, 20 & 30 mm on AA6061-T6 alloy at the rotational speeds of 400, 800, 1200 and 1600 rpm are shown in Figure 10. It is clear that a softened region consisting of the NZ, TMAZ and HAZ were created in all the normal and underwater FSW joints. Liu Hui-jietai.¹³ were found that the submerged friction stir joint has a lower hardness in the WNZ and higher hardness in the TMAZ and HAZ. Abnormal control of hardness values was reported by

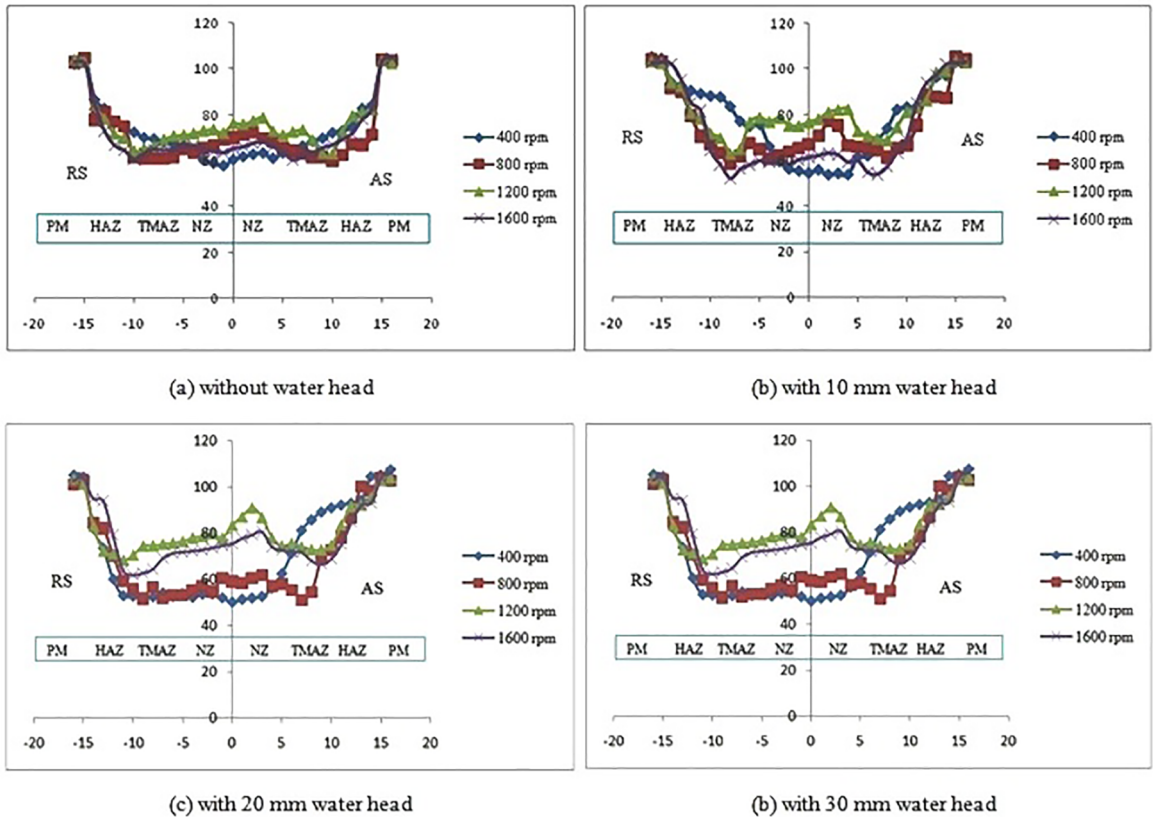


Figure 10 . Hardness profiles (a) without water head (b) with 10 mm water head (c) with 20 mm water head (d) with 30 mm water head

precipitate distribution, solid solution, dislocation density and grain size.

The microhardness curve of “U” shape was found at the low rotational speed of 400 rpm in both normal and submerged friction stir welding due to the low heat generation. At last, lower hardness values were found at the rotational speed of 400 rpm in friction/submerged friction stir welding process. Zhang et al.¹⁶ were found the lower hardness in the nugget zone due to the strain hardening of the low-density dislocations as insufficient and improving to the strength loss of the welded plates at the lower rotational speed of 600 rpm.

The “W” shape of microhardness profiles is attained from the rotational speed of 800 to 1600 rpm in both joints. The max. average hardness of the friction and submerged friction joint with various water heads was 75.29, 78.74, 83.56, and 79.31 Hv respectively in the weld Nugget Zone (WNZ). The max. average hardness was found to be 68.85, 72.45, 74.84 and 73.57 Hv in the thermo-mechanically affected zone (TMNZ) of friction and submerged friction stir joints of various water heads. The hardness value of WNZ and TMAZ increased up to the rotational speed of 1200 rpm, followed by a decrease in 1600 rpm. Finally, higher hardness values are attained at the rotational speed of 1200 rpm in SFSW with a water head of 20 mm as result of formation a very fine grain structure.

3.6 Microstructural analysis

The mechanical properties like tensile and hardness depend on the microstructural characteristics of the welded sample. Selected samples were observed under the scanning electron microscopy on Hitachi S-3000N equipment. In this work, the maximum Avg. hardness and ultimate tensile strength were observed at the rotational speed of 1200 rpm.

A total of five samples were taken for metallographic analysis in the rotational speed of 1200 rpm, in which three samples are taken from submerged friction stir welding process at the water head of 10, 20 & 30 mm, one sample as normal friction stir welding process and again one sample as the parent material. Fig. 11 shows microstructure of the parent metal of 6061-T6 aluminium alloy, which contains coarser elongated grains along with the rolling direction and grain size of 98.24 μm . The variation of average grain size (μm) was measured using image-J analysis software on the weld nugget zone of welded plates produced under the water head of 10, 20 & 30 mm and without water head (normal FSW) at the rotational speed rates of 1200 rpm are presented in Fig. 12 (b-d). The avg. grain size (μm) of 20.96, 10.58, 5.32 and 9.04 are attained in normal and submerged friction stir welding of 10, 20 and 30 mm water head respectively.

The grain size is higher in normal friction stir welding process when compared to the submerged friction welding process due to the generation of excess heat, and it plays

the predominant role in grain size. But, the significant grain refinement was also achieved during the friction stir welding process; furthermore, the average grain size was decreased from 98.24 μm to 20.96 μm . Douglas et al.²⁷ conducted experiments of friction stir processing in their

and submerged friction stir processing under the liquid of Al6061-T6. The grain size of the Al6061-T6 aluminium alloy was approximately 50 μm . The approximate grain sizes of 5 μm and 2 μm were identified in FSP and SFSP respectively. They have concluded that SFSP is an enhanced method of FSP which creates the ultrafine grains.

In submerged friction stir processing, the grain size was found to be higher in water head of 10 mm when compared to the water head of 30 mm. Because the maximum water temperature of 49.8°C, 43.8°C, and 40.9°C were identified during the submerged friction stir welding condition at the water head of 10, 20 and 30 mm. The maximum water temperature is high during the water head of 10 mm compared to the water head of 20 mm and 30 mm during which the quantity of water is low. Very fine grain size was attained in the submerged friction stir welding of 20 mm water head. In this condition, the thermal cycle (heating and cooling) of the weld is expected as optimized. This may have led to the decrease in grain size.

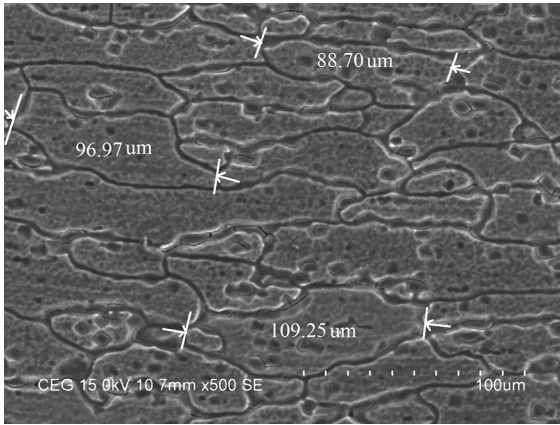
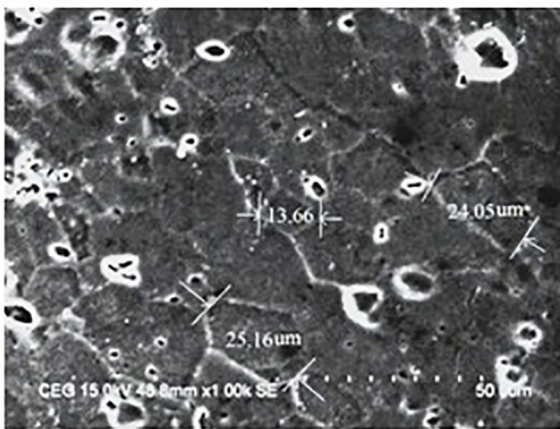
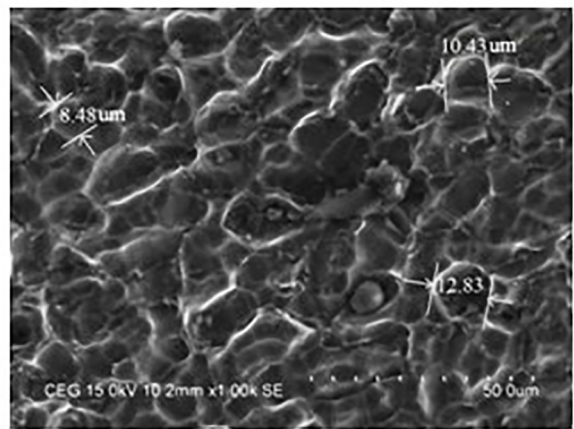


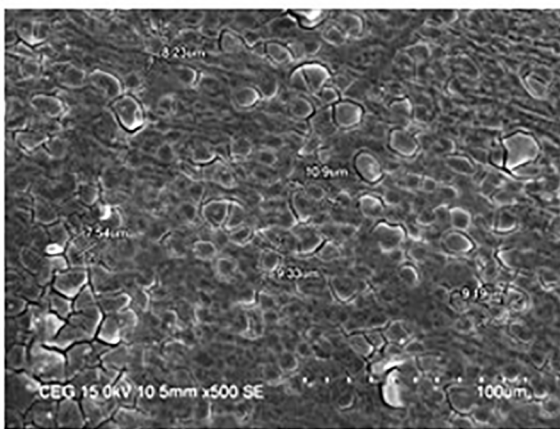
Figure 11 . Microstructures of the parent metal



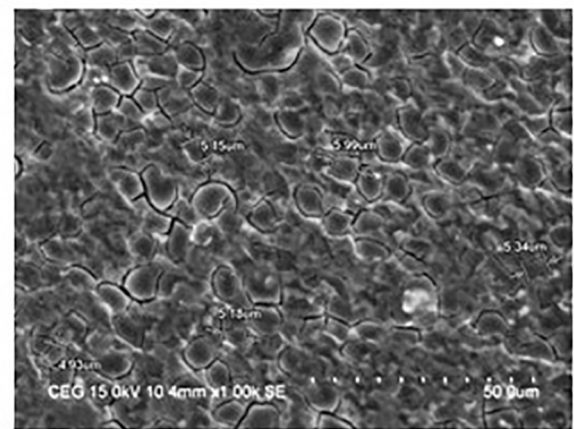
(a) without water head



(b) with 10 mm water head



(c) with 20 mm water head



(d) with 30 mm water head

Figure 12 . Scanning electronmicrographs of the SZ (a) without water head (b) with 10 mm water head (c) with 20 mm water head (d) with 30 mm water head

3.7 Comparisons study of FSW and SFSW

A comparison between friction and submerged friction stir welding at the various water heads of 10, 20 & 30 mm on 6061-T6 aluminium alloy is shown in Table 3.

A look at the data in Table 3 shows that the torque generation and power consumption of submerged friction stir welds at the low water head of 10 mm and seen increasing by 57.69% and 56.56% respectively when compared to the normal friction stir welding. The maximum tensile strength is increased by 3.22 % on submerged friction stir welds at the water head of 20 mm, when compared to the submerged friction stir welds at the water head of 30 mm. The average hardness value in nugget zone of SFSW at the water head of 20 mm was 5.81% higher than the water head of 10 mm. The average hardness value of the thermo-mechanically affected zone is increased by 1.7 % of SFSW at a water head of 20 mm, when compared to 30 mm water head. The grain size diminished in SFSW at the water head of 20 mm to 294 %, when compared to the normal friction stir welding sample. The grain size diminished by 69.93 % on submerged friction stir welds, at the medium water head to low water head.

Table 3. Comparisons of performance between FSW and SFSW

Performance	Comparisons	Increased by (%)
Torque (Nm)	^c SFSW > ^b SFSW	1.05
	^b SFSW > ^a SFSW	5.92
	^a SFSW > FSW	57.69
Power (kW)	^c SFSW > ^b SFSW	3.58
	^b SFSW > ^a SFSW	1.86
	^a SFSW > FSW	56.61
Tensile strength (MPa)	^b SFSW > ^c SFSW	3.22
	^c SFSW > ^a SFSW	1.9
	^a SFSW > FSW	12.08
Microhardness (Hv) in NZ	^b SFSW > ^a SFSW	5.81
	^a SFSW > FSW	4.39
	FSW > ^c SFSW	8.56
Microhardness (Hv) in TMAZ	^b SFSW > ^c SFSW	1.7
	^c SFSW > ^a SFSW	1.53
	^a SFSW > FSW	4.97
Average grain size (µm) in NZ	FSW > ^c SFSW	49.53
	^a SFSW > ^c SFSW	14.56
	^c SFSW > ^b SFSW	41.16

^aSFSW - Submerged friction stir welding for 10 mm water head; ^b

^bSFSW - Submerged friction stir welding for 20 mm water head; ^c

^cSFSW - Submerged friction stir welding for 30 mm water head;

FSW – Friction stir welding for without water head.

4. Conclusion

The findings of this investigation are:

- Torque and power consumptions increase following an increase in the water head during the submerged friction stir welding. The torque values and power consumption are high in the submerged friction stir welding compared to the normal friction stir welding.
- The superior weld morphology as onion ring pattern is achieved during the submerged friction stir welding process and it is not present in the friction stir welded samples.
- The working range of the friction stir welding process parameter of rotational speed is 800 to 1200 rpm and for submerged friction stir welding varies from 800 to 1600 rpm which is determined by macrostructure analysis for defect-free samples.
- Compared with the normal friction stir welding, the submerged friction stir welding exhibits higher tensile strength. The maximum tensile strength increases by 16.52 % on submerged friction stir welds (water head of 20 mm), when compared to the normal friction stir welds.
- Submerged friction stir welding exhibits higher microhardness in the TMAZ and WNZ when compared to the normal FSW joint. The maximum microhardness in the TMAZ and NZ increases by 8% and 9.93 % respectively under submerged friction stir welds of 20 mm water head when compared to the normal friction stir welds.
- The fine grain size was achieved in submerged friction stir welding at the water head of 20 mm due to the proper heating and cooling effect.

5. Acknowledgement

The authors are grateful to the University Grants Commission (UGC), New Delhi, India for granting funds through project no. RGNF-2015-17-TAM-1232.

6. References

1. Mishra RS, Ma ZY. Friction stir welding and processing. *Materials Science and Engineering: R: Reports*. 2005;50(1-2):1-78.
2. Rajakumar S, Muralidharan C, and Balasubramanian V. Establishing empirical relationships to predict grain size and tensile strength of friction stir welded AA 6061-T6 aluminium alloy joints. *Transactions of Nonferrous Metals Society of China*. 2010;20:1863-1872.

3. Rathinasuriyan C, Senthil Kumar VS, Shanbhag AV. Radiography and Corrosion Analysis of Sub-merged Friction Stir Welding of AA6061-T6 alloy. *Procedia Engineering*. 2014;97:810-818.
4. Lokesh R, Senthil Kumar VS, Rathinasuriyan C, Sankar R. Optimization of process parameters: Tool pin profile, rotational speed and welding speed for submerged friction stir welding of AA6063 alloy. *International Journal of Technical Research and Applications*. 2015;12:35-38.
5. Zhang J, Shen Y, Yao X, Xu H, Li B. Investigation on dissimilar underwater friction stir lap welding of 6061-T6 aluminum alloy to pure copper. *Materials & Design*. 2014;64:74-80.
6. Wang Q, Zhao Y, Yan K, Lu S. Corrosion behavior of spray formed 7055 aluminum alloy joint welded by underwater friction stir welding. *Materials & Design*. 2015;68:97-103.
7. Zhang, H. and Liu, H. Characteristics and formation mechanisms of welding defects in underwater friction stir welded aluminum alloy. *Metallography, Microstructure, and Analysis*. 2012; 1(6):269-281.
8. Rathinasuriyan C, Senthil Kumar VS. Submerged Friction Stir Welding and Processing: Insights of Other Researchers. *International Journal of Applied Engineering Research*. 2015;10(8):6530-6536.
9. Su H, Wu CS, Pittner A, Rethmeier M. Simultaneous measurement of tool torque, traverse force and axial force in friction stir welding. *Journal of Manufacturing Processes*. 2013;15(4):495-500.
10. Jonckheere C, de Meester B, Denquin A, Simar A. Torque, temperature and hardening precipitation evolution in dissimilar friction stir welds between 6061-T6 and 2014-T6 aluminum alloys. *Journal of Materials Processing Technology*. 2013;213(6):826-837.
11. El-Hafez HB. Mechanical Properties and Welding Power of Friction Stirred AA2024-T35 Joints. *Journal of Materials Engineering and Performance*. 2011;20(6):839-845.
12. Lakshminarayanan AK, Malarvizhi S, Balasubramanian V. Developing friction stir welding window for AA2219 aluminium alloy. *Transactions of Nonferrous Metals Society of China*. 2011;21(11):2339-2347.
13. Liu H, Zhang H, Huang Y, Yu L. Mechanical properties of underwater friction stir welded 2219 aluminum alloy. *Transactions of Nonferrous Metals Society of China*. 2010;20(8):1387-1391.
14. Darras B, Kishta E. Submerged friction stir processing of AZ31 Magnesium alloy. *Materials & Design*. 2013;47:133-137.
15. Zhang H, Liu H. Mathematical model and optimization for underwater friction stir welding of a heat-treatable aluminum alloy. *Materials & Design*. 2013;45:206-211.
16. Kishta EE, Darras B. Experimental investigation of underwater friction-stir welding of 5083 marine-grade aluminum alloy. *Proceedings of the Institution of Mechanical Engineers, Part B: Journal of Engineering Manufacture*. 2016;230(3):458-465.
17. Zhang HJ, Liu HJ, Yu L. Microstructure and mechanical properties as a function of rotation speed in underwater friction stir welded aluminum alloy joints. *Materials & Design*. 2011;32(8-9):4402-4407.
18. Liu HJ, Zhang HJ, Yu L. Effect of welding speed on microstructures and mechanical properties of underwater friction stir welded 2219 aluminum alloy. *Materials & Design*. 2011;32(3):1548-1553.
19. Gao J, Shen Y, Xu H. Investigations for the mechanical, macro-, and microstructural analyses of dissimilar submerged friction stir welding of acrylonitrile butadiene styrene and polycarbonate sheets. *Proceedings of the Institution of Mechanical Engineers, Part B: Journal of Engineering Manufacture*. 2016;230(7):1213-1220.
20. Bloodworth T. *On the Immersed Friction Stir Welding of AA6061-T6: A Metallurgic and Mechanical Comparison to Friction Stir Welding*. [Thesis]. Nashville: Vanderbilt University; 2009.
21. Puviyarasan M, Senthil Kumar VS. Optimization of friction stir process parameters in fabricating AA6061/SiCp composites. *Procedia Engineering*. 2012;38:1094-1103.
22. Givi MKB, Asadi P. *Advances in Friction Stir Welding and Processing*. Cambridge: Woodhead Publishing; 2014.
23. Lakshminarayanan AK, Balasubramanian V. Comparison of RSM with ANN in predicting tensile strength of friction stir welded AA7039 aluminium alloy joints. *Transactions of Nonferrous Metals Society of China*. 2009;19(1):9-18.
24. Elatharasan G, Senthil Kumar VS. An Experimental Analysis and Optimization of Process Parameter on Friction Stir Welding of AA 6061-T6 Aluminum Alloy using RSM. *Procedia Engineering*. 2013;64:1227-1234.
25. Cui GR, Ma ZY, Li SX. Periodical plastic flow pattern in friction stir processed Al-Mg alloy. *Scripta Materialia*. 2008;58(12):1082-1085.
26. Yoon TJ, Yun JG, Kang CY. Formation mechanism of typical onion ring structures and void defects in friction stir lap welded dissimilar aluminum alloys. *Materials and Design*. 2016;90:568-578.
27. Hofmann DC, Vecchio KS. Submerged friction stir processing (SFSP): An improved method for creating ultra-fine-grained bulk materials. *Materials Science and Engineering: A*. 2005;402(1-2):234-241.